Neutron Reflectometry Study of Surface Segregation in an Isotopic Poly(ethylenepropylene) Blend: Deviation from Mean-Field Theory

L. J. Norton[†] **and E. J. Kramer***

Department of Materials Science and Engineering, and Materials Science Center, Cornell University, Ithaca, New York 14853

F. S. Bates and M. D. Gehlsen[‡]

Department of Chemical Engineering and Materials Science, University of Minnesota, Minneapolis, Minnesota 55455

R. A. L. Jones

Cavendish Laboratory, Madingley Road, Cambridge, UK CB3 OHE

A. Karim

National Institute of Standards and Technology, Gaithersburg, Maryland 20899

G. P. Felcher and R. Kleb

Materials Science Division, Argonne National Laboratory, Argonne, Illinois 60439

Received April 10, 1995; Revised Manuscript Received August 15, 1995[⊗]

ABSTRACT: Neutron reflectometry (NR) was used to measure the concentration profile of a symmetric PEP/dPEP polymer blend with nanometer-scale resolution in the one-phase region. The shape of the profile near the surface was found to differ significantly from mean-field theory predictions for all bulk concentrations and temperatures surveyed. The profile shape is flattened at the surface over a distance about half the bulk correlation length, a length scale far greater than that of the dispersive forces that are the dominant microscopic interaction in such blends. We introduce a new method for extracting the surface energy difference that drives segregation based on the Gibbs adsorption equation (GAE) and compare it to a previous method based on mean-field theory. While both methods produce qualitatively similar results (the surface energy of pure dPEP is ~0.21 mJ/m^2 smaller than pure PEP), the GAE method is much less model dependent, requiring knowledge of only the free energy of mixing in the bulk and the measured integral excess and surface composition. The surface energy difference between dPEP and PEP is ~2.6 times larger than that for dPS and PS, a factor in good agreement with the expectation that the surface energy difference between the isotopically different polymers arises from the same van der Waals interaction that leads to a positive Flory segment–segment interaction parameter χ in these blends.

Introduction

The chemical composition at the surface of a mixture can have important consequences for the surface properties of a material. A fundamental understanding of the thermodynamics of surfaces enables the tailoring of surface properties for specific applications. In polymer mixtures, the entropy of mixing of long-chain molecules is small and often of a magnitude comparable to the interactions between blend components or between the individual polymers and a surface. In such cases, the thermodynamics often favors segregation, or more dramatically phase separation, of the low surface energy component to a surface. Mixtures of structurally equivalent pairs of homopolymers that differ only in their isotopic composition of their hydrogen/deuterium content form model nonideal mixtures for sufficiently long molecules.[1–3] The small unfavorable interaction, characterized by a small positive segment–segment interaction parameter χ between the two isotopic species, is a consequence of the slight difference in bond length and polarizability between the C–H and the C–D bonds. For sufficiently large molecules, the relatively small combinatorial entropy of mixing can produce a miscibility gap with an upper critical solution temperature. Deuteration also creates a small difference in surface energy between the two components. In polymer blends of equal chain lengths, segregation of the lower surface energy component, the deuterated polymer, occurs when the energetic cost of having a surface layer with an off-equilibrium composition accompanied by a composition gradient is outweighed by the reduction in surface energy. The amount of enrichment and the shape of the depth profile are governed by this trade-off.

The first theories[4,5] developed to describe the shape of the surface enriched layer with depth relied on the minimization of the excess surface free energy per lattice site, F_s

$$\frac{F_s(\phi(z))}{k_B T} = f_s + \int_0^\infty dz\left[G(\phi) - \Delta\mu\phi + \frac{a^2}{36\phi(1-\phi)}\left(\frac{d\phi}{dz}\right)^2\right] \quad (1)$$

The free energy of mixing per lattice site is given by $G(\phi) = [\phi/N_d] \ln \phi + [(1-\phi)/N_h] \ln (1-\phi) + \chi\phi(1-\phi)$ where $\Delta\mu = \delta G/\delta\phi$ evaluated at the bulk composition

[†] Current address: Motorola, 1300 N. Alma School Rd., CH200, Chandler, AZ 85224.

[‡] Current address: 3M Center, Bldg 208-01-01, St. Paul, MN 55144-1000.

[⊗] Abstract published in *Advance ACS Abstracts,* October 15, 1995.

0024-9297/95/2228-8621$09.00/0

ϕ_∞. The composition dependence on depth is denoted with $\phi(z)$, the statistical segment length is given by a, the polymerization indexes are N_h and N_d, and k_BT is the Boltzmann constant multiplied by the temperature. The entropic penalty associated with sharp gradients in composition is expressed as a term proportional to the square of the composition gradient; this so-called "square gradient approximation" is valid in the limit where such gradients are small compared to the size of the polymer coil. The bare surface energy f_s within this framework depends only on the concentration at the surface, ϕ_1, a zero-range surface interaction, as

$$f_s = -\mu_1\phi_1 - \frac{1}{2}g{\phi_1}^2 \tag{2}$$

with μ_1 describing the chemical potential favoring one component at the surface and g accounting for the missing interactions of segments at the surface. The composition profile that minimizes F_s follows the functional form

$$z = \frac{a}{6}\int_{\phi_1}^{\phi(z)} \frac{d\phi}{\sqrt{\phi(1-\phi)[G(\phi) - G(\phi_\infty) - \Delta\mu(\phi - \phi_\infty)]}} \tag{3}$$

which has an exponential-like decay from the surface concentration ϕ_1 to the bulk concentration ϕ_∞ when the ϕ_∞ is far from the binodal composition. Measurements of ϕ_1, or alternatively the integrated surface excess defined as $z^* = \int_0^\infty[\phi(z) - \phi_\infty]\,dz$, as a function of ϕ_∞ for a system where the bulk thermodynamics are known through χ allows determination of the bare surface energy derivative[6] that drives the surface segregation

$$\frac{d\gamma_b}{d\phi_1} = \frac{k_BT}{b^3}\frac{df_s}{d\phi_1} \tag{4}$$

where b^3 equals the segment volume. From eq 1 an expression for $df_s/d\phi_1$ is derived as

$$-\frac{df_s}{d\phi_1} = \frac{a}{3}\sqrt{\frac{G(\phi_1) - G(\phi_\infty) - \Delta\mu(\phi_1 - \phi_\infty)}{\phi_1(1-\phi_1)}} \tag{5}$$

We will refer to the above as the SB mean-field theory after the authors of ref 5.

A variety of polymer blends have been studied using a diverse set of profiling tools,[7-13] in some cases experimentally testing this theory, and general agreement has been found. However, in miscible blends of polystyrene and deuterated polystyrene (PS/dPS), the more highly segregated samples were observed to have a region of constant concentration near the surface before the profile decayed with an exponential-type form to the bulk concentration.[9,10] One explanation that was proposed to explain the thicker surface layer was the presence of long-range forces. To experimentally test this hypothesis and separate the contribution to the profile shape of chain configuration from the surface interactions, we have chosen another isotopic blend that offers a number of advantages.

Poly(ethylenepropylene) (PEP) blended with its deuterated analogue (dPEP) has a high D/C or H/C ratio and therefore the interactions, described by χ, dominate the thermodynamics for much lower chain lengths than for other familiar polymers such as PS. Blends of PEP/dPEP have been extensively studied and characterized with small-angle neutron scattering (SANS). Near the critical point for phase separation in a series of blends of symmetric chain length, the segment–segment interaction parameter follows the temperature dependence[14]

$$\chi = \left(\frac{\Delta x_d}{10}\right)^2\left[\frac{0.571 \pm 0.007}{T} - (6.56 \pm 0.18) \times 10^{-4}\right] \pm 2 \times 10^{-5} \tag{6}$$

where Δx_d is the difference between the number of D atoms per monomer unit on the dPEP and on the PEP chains. We pursued an investigation with neutron reflectometry of the detailed shape of the surface segment density profile in PEP/dPEP blends as a function of composition and temperature.

Experiment

(1) Materials and Sample Preparation. Poly(ethylene propylene) and its deuterated analogue were prepared by hydrogenating anionically polymerized 1,4-polyisoprenes.[15] The two components had nearly equal lengths with a weight-average degree of polymerization $N_{PEP} = 2360$ and $N_{dPEP} = 2140$ and a polydispersity index of less than 1.04. Thin films of varying bulk compositions of dPEP were prepared as follows. Polished silicon wafers (5 mm thick and either 2.5 or 5 cm in diameter) were cleaned to remove organic contaminants using a room temperature etch solution of ~8:1 sulfuric acid and hydrogen peroxide. This chemical cleaning was followed by reactive ion etching in an oxygen plasma. The silicon oxide, whose high neutron scattering length density can complicate the analysis of the reflectivity spectra, was stripped with a buffered HF solution (pH between 5 and 6) followed by a thorough rinse in deionized water.[16] The stripped silicon surface was then immediately spin coated with PEP/dPEP co-dissolved in toluene to achieve a film thickness $L \approx 1500$ Å, ~10 times the radius of gyration ($R_g = a\sqrt{N/6}$ where $a \approx 8$ Å with $\ln a^2 = -1.0 \times 10^{-3}T \pm 4.48$ [17]). The samples were annealed at either 70 or 35 °C by being placed at the bottom of a container that was sealed in air and then partially immersed in a water bath. To achieve equilibrium surface segregation profiles, annealing times were used that produced a diffusion distance w ($w = (4Dt)^{1/2}$, where t is time and D is the diffusion coefficient) of at least $35L$ based on previously measured diffusion coefficients for these polymers.[18,19] The samples were cooled within ~4 min to a temperature −55 °C, the glass transition temperature of PEP, and neutron reflection experiments were carried out at this temperature to avoid any change in the composition profile during measurement.

(2) Neutron Reflectometry. Neutron reflectometry (NR) probes the scattering length density profile $(b/V)(z)$ perpendicular to the film surface. The scattering length density $(b/V)(z)$ depends on the density and type of nuclei within a small-volume element. The large contrast between the scattering length of H and D permits isolation of the segment density distribution of dPEP in PEP with depth from $(b/V)(z)$. The NR measurements were performed on the POSYII beam line at the Intense Pulsed Neutron Source at Argonne National Laboratory.[20] The technique is presented elsewhere in an excellent review.[21] The wavelength λ distribution in each incident pulse of neutrons ranges from 3 to 14 Å. Since the reflectivity R is measured as a function of the perpendicular component of the incident wavevector, $k = (2\pi/\lambda)\sin(\theta)$, several incident angles θ were used to measure $R(k)$ up to $k = 0.05$ Å^{-1}. Fits to the data were determined by first assuming a $(b/V)(z)$ and then approximating it by a series of uniform layers where the change in scattering length density, $\Delta(b/V)$, between successive layers was kept constant and finally calculating R using a standard multilayer algorithm.[21,22] These steps were repeated until good agreement between the simulation and the data was reached through a minimization of the χ_{err}^2 in each angular data set, defined as

$$\chi_{err}^2 = \frac{1}{n}\sum_{i=1}^{n}\frac{(R_{m,i} - R_{c,i})^2}{\sigma_i^2} \tag{7}$$

Table 1. Neutron Scattering Length Density

material	b/V ($\times 10^{-6}$ Å^{-2})
dPEP	7.38
hPEP	−0.306
Si	2.08

where R_m and R_c are the measured and calculated reflectivities, respectively, σ_i is the standard deviation error of R_m, and n is the number of data points in a data set taken at a particular incident angle. In addition, the amount of PEP and dPEP of the simulation was matched to the total content of the initial uniform film taking into account the depletion of the bulk concentration below the initial film concentration. Values of b/V used to convert the $(b/V)(z)$ to $\phi(z)$ are listed in Table 1. To account for incoherent scattering from the hydrogen-containing polymers, an imaginary component of the scattering length density $b/V|_i$ was included in the profiles. This loss mechanism provides an important constraint to the determination of $(b/V)(z)$ through the position and depth of dips in R at k below the critical wavevector for total reflection k_c. These features are caused by resonantly enhanced neutron standing waves in the potential well formed between the high b/V surface layer and the Si.[23,24] The roughness (rms) of the silicon substrate was fixed at 5 Å.[9] The polymer surface roughness was used as a fitting parameter and was found to lie between 7 and 13 Å for all samples, agreeing with both X-ray reflectometry and atomic force microscopy measurements.[25] Segregation to the stripped silicon surface was not included in our fits. It has been observed in direct space profiling of surface-directed spinodal decomposition in thin films that the PEP is attracted to the silicon interface.[26,27] However, since the bulk compositions are low ($\phi_\infty < 0.15$), we expect only a small change in dPEP concentration near the silicon, if any. The functional form of the composition profile used to fit these data is discussed in detail in an appendix with important parameters presented in the following section.

Results

In Figure 1 the reflectivity data are shown for a film, 1614 Å thick, of a blend of PEP/dPEP annealed at 70 °C. The thick solid line through the data is $R(k)$ calculated from the best-fit scattering length density profile shown in the inset with a thick solid line. The thin line fit is obtained from the mean-field prediction (eq 3) by taking χ from eq 6 and matching the surface and bulk dPEP concentrations of the best fit. In Figure 2, $(b/V)(z)$ for all the samples annealed at 70 °C have been converted to $\phi(z)$. From the profile corresponding to the data of Figure 1, we see that a bulk concentration of dPEP of $\phi_\infty = 0.126$ is in equilibrium with an enriched surface with a surface concentration $\phi_1 = 0.83$ (Figure 2b). Assuming the same value of ϕ_1, the measured integrated surface excess of dPEP, z^*, is considerably larger than that predicted with eq 3. In addition, the shape of the profile has a noticeably different feature. Instead of decreasing exponentially with z at short distances from the surface, $\phi(z)$ remains nearly constant to a depth of ~50 Å and only reaches the form of the mean-field prediction asymptotically at large z. The profiles for samples annealed at 35 °C are presented in Figure 3 with the associated profiles predicted from mean-field theory. At both temperatures, the best fits were found when a thick surface layer was added to the profile predicted from mean-field theory with the thickness of the flattened region generally decreasing as ϕ_∞ is decreased.

To check our annealing time criterion for equilibrium, the neutron reflectivity data were measured from two films prepared from the same solution of initial concentration $\phi_0 = 0.314$. One sample was annealed at 70 °C for 3 days and the other for 12 days. No statistically significant difference in the reflectivity data of the two

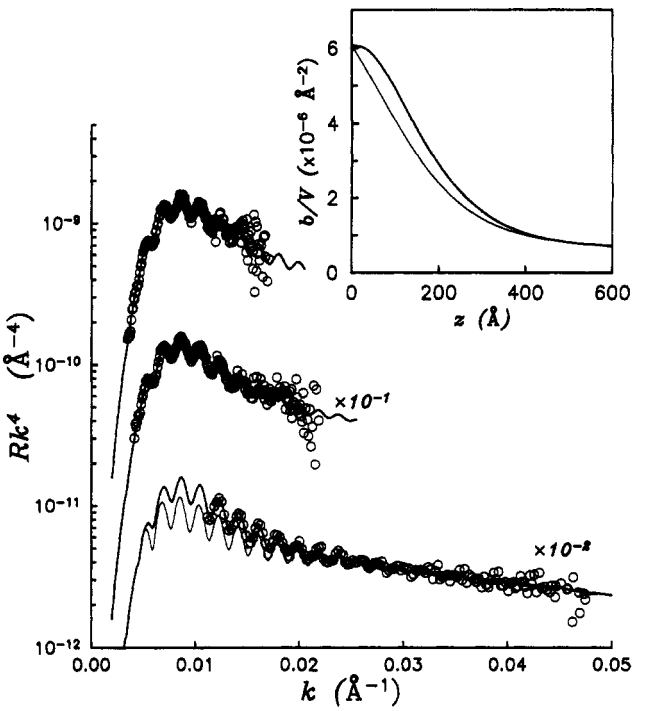

Figure 1. Neutron reflectivity data for a sample with $\phi_\infty = 0.126$ annealed at 70 °C for 10 days. Data (circles) obtained at different incident angles are offset by factors of 10 for clarity and the fits adjusted for changes in instrumental resolution. The thick solid line represents the calculated reflectivity using the scattering length density profile shown in the inset with a thick line. The thin lines correspond to the reflectivity (shown only for one data set) and the associated scattering length density profile of eq 3.

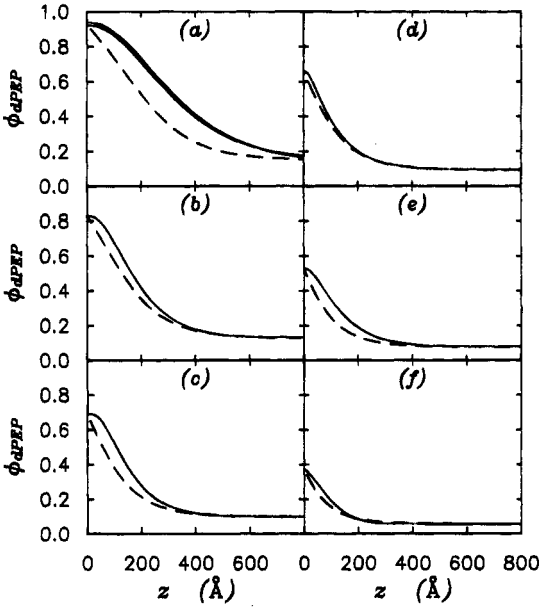

Figure 2. Measured volume fraction dPEP depth profiles (solid lines) for samples annealed at 70 °C with different bulk concentrations: (a) $\phi_\infty = 0.149$ annealed 12 days (thick line) and $\phi_\infty = 0.130$ annealed 3 days (thin line), (b) $\phi_\infty = 0.126$, (c) $\phi_\infty = 0.099$, (d) $\phi_\infty = 0.091$, (e) $\phi_\infty = 0.075$ and (f) $\phi_\infty = 0.053$. Other annealing times given in Table 2. Dashed lines are computed with eq 3.

films was observed, indicating that 3 days of annealing at 70 °C was sufficient for the films to reach equilibrium. The two profiles are shown in Figure 2a, both of which conserve dPEP and have $\chi_{err}^2 < 6$ for each angle (see Table 2). The barely discernible differences in the profiles of these two samples are presented to give a flavor for the error in the fitting the samples with a

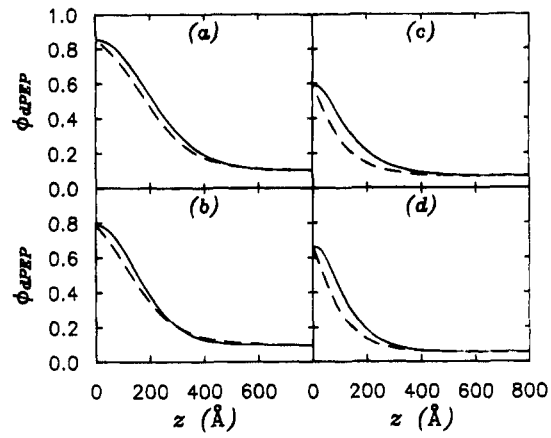

Figure 3. Measured dPEP volume fraction depth profiles (solid lines) for samples annealed at 35 °C for 15 days with different bulk concentration: (a) $\phi_\infty = 0.098$, (b) $\phi_\infty = 0.094$, (c) $\phi_\infty = 0.066$, and (d) $\phi_\infty = 0.054$. Profiles computed using eq 3 (dashed line).

Table 2. Fitting Parameters[a]

ϕ_∞	ϕ_1	z^* (Å)	L (Å)	t (days)	χ_{err}^2
			At 35 °C		
0.098	0.854	183	1679	15	2.7, 1.8, 1.6
0.094	0.789	134	1996	15	2.7, 2.0, 1.5
0.066	0.591	84	1563	15	3.5, 3.3, 1.7
0.054	0.665	85	1893	15	2.1, 1.8, 1.3
			At 70 °C		
0.149	0.924	273	1552	12	5.4, 2.7, 1.5
0.130	0.940	287	1530	3	3.4, 2.2, 2.3
0.126	0.831	139	1614	10	2.0, 2.1, 1.3
0.099	0.691	98	1622	10	3.1, 1.9, 1.8
0.091	0.634	72	1547	1.83	7.7, 3.2, 2.8
0.075	0.530	67	1541	10	2.5, 1.2, 1.1
0.053	0.391	37	1699	3	2.0, 1.8

[a] Where ϕ_∞ is the bulk volume fraction of *dPEP*, ϕ_1 is the surface volume fraction of *dPEP*, L is the film thickness, t is the annealing time, and χ_{err}^2 is defined by eq 7 for each angular data set.

Table 3. Fitting Parameters (continued) Defined in Equations 24 and 26

ϕ_∞	λ_1 (Å)	λ_2 (Å)	λ_{max} (Å)	β
		At 35 °C		
0.098	36	1.41×10^6	1.04×10^4	0.458
0.094	35	1.20×10^5	7.27×10^3	0.452
0.066	95	1.72×10^9	7.60×10^3	0.276
0.054	71	5.92×10^7	5.60×10^3	0.312
		At 70 °C		
0.149	100	1.13×10^6	1.37×10^4	0.419
0.130	115	1.13×10^6	1.21×10^4	0.411
0.126	78	2.60×10^5	4.58×10^3	0.375
0.099	78	7.46×10^8	1.02×10^4	0.287
0.091	102	1.6×10^{21}	8.25×10^3	0.121
0.075	82	2.41×10^6	4.11×10^3	0.387
0.053	94	9.46×10^{18}	5.09×10^3	0.142

thick surface layer when the reflectivity is only weakly sensitive to the bulk concentration. Profiles that did not include this nearly constant concentration of dPEP near the surface could not fit the data between $k = k_c$ and $k \approx 0.02$ Å^{-1} while simultaneously fitting the highest k data measured.

The profile fitting parameters are summarized with two plots. In Figure 4, the integrated surface excess of dPEP, z^*, is plotted versus ϕ_∞. There is a systematic increase in z^* as ϕ_∞ approaches the binodal composition computed from χ found with SANS (eq 6) and Flory–Huggins theory. The surface composition ϕ_1 also increases with ϕ_∞ (Figure 5) and decreases when the annealing temperature is raised. The experimental results follow the expectation that as the miscibility of

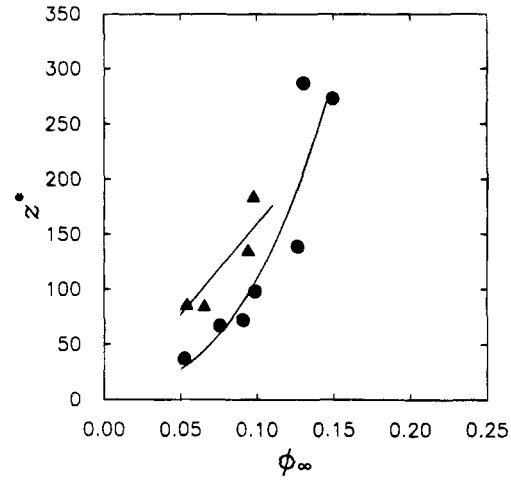

Figure 4. Surface excess versus bulk concentration of dPEP for samples annealed at 70 (circles) and at 35 °C (triangles). Lines are provided as a guide to the eye.

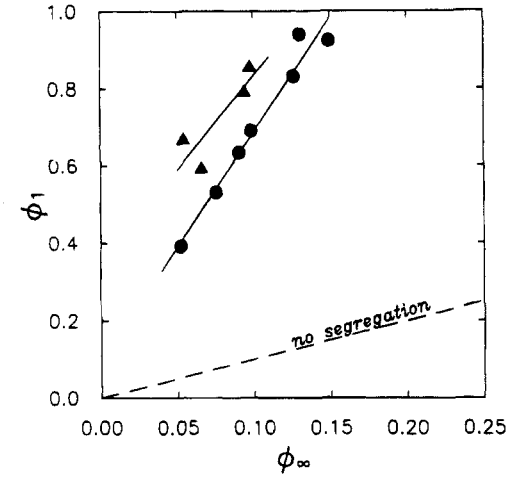

Figure 5. Surface volume fraction of dPEP versus bulk concentration of dPEP for samples annealed at 70 (circles) and at 35 °C (triangles). Lines are provided as a guide to the eye.

dPEP in PEP improves (higher temperature) or as ϕ_∞ is lowered, the surface concentration and the total amount of dPEP at the surface decreases.

Discussion

(1) Surface Segregation Profile. One noticeable feature of the surface segregation profiles brought to light by the high sensitivity of the NR probe and by the large surface energy difference of the PEP/dPEP system relative to other isotopic blends (e.g., PS/dPS) is the extent of deviation from mean-field theory. In PS/dPS measured with both secondary ion mass spectrometry (SIMS)[10] and NR,[9] samples with large ϕ_∞ have been observed to have a broader profile than the SB prediction, similar to our results. The suggestion[28] that long range surface interactions might account for this deviation was tested quantitatively by Jones.[29] The excess surface free energy expression (eq 1) was modified by the addition of a term to model a van der Waals surface interaction decaying with depth as z^{-3}. Numerical integration of the Euler–Lagrange equation resulting from the minimization of this expanded surface free energy expression revealed that profiles were only modified within the first 5 Å, for a polymer blend with characteristics similar to the long-chain PS/dPS where marked broadening was observed.[9,10] These differences are not experimentally accessible to either NR and SIMS and do not account for the flattening we observe

that approaches the radius of gyration of the polymers in the PEP/dPEP blend.

A self-consistent mean-field theory of surface segregation (SCF)[30] has been constructed that removes the square gradient approximation in eq 1 but retains the mean-field approximation. With material characteristics of PS/dPS, the SCF calculations produced a near-surface profile with only a slightly more gradual decay than the SB prediction approaching the SB shape far from the surface. When a long-range surface force of the same functional form as Jones studied was included in the SCF theory,[31] no change in the profile was seen similar to near-surface flattening observed in PS/dPS.[9,10] Using the material parameters that describe the PEP/dPEP blend, the SCF simulations were unable to match the magnitude of the deviation from the mean-field prediction[32] that we have observed with the high-resolution NR technique.

Several theories modify the excess surface free energy F_s, improving on the phenomenological assignment of the form of f_s in the SB theory (eq 2).[33,34] Terms of these new expressions describe aspects of the surface such as the entropic configuration of the lattice sites. The importance of such entropic contributions to the segregation thermodynamics has been observed in experiments investigating symmetric polyolefin diblock copolymers.[35] In these systems, the surface energy difference between blocks, for example, PEP – dPEE where PEE is poly(ethylethylene), was of the same order as in our studies. It was the more flexible block, with the shorter statistical segment length a, that segregated to the surface or interface, agreeing with predictions that address this aspect of the chain architecture.[36] This asymmetry in a is not present in our studies of PEP/dPEP, and it is the energetic difference between the segments that dominates. The bulk free energy is not modified at all by these treatments of surface segregation just mentioned, and it is the bulk free energy terms that determine the decay of the profile away from the surface. The modification of the f_s term in the SB theory thus will not be able to account for the near-surface flattening that we see in PEP/dPEP.

In Figure 6, typical profiles for two different temperatures are plotted as a function of normalized depth, i.e., z scaled by the bulk correlation length ξ which is given by

$$\xi = \frac{a}{6}\frac{1}{\sqrt{\phi_\infty(1-\phi_\infty)(\chi_s - \chi)}} \tag{8}$$

and where χ_s is the value of χ at the spinodal, i.e.

$$\chi_s = \frac{1}{2}\left(\frac{1}{N_d\phi_\infty} + \frac{1}{N_h(1-\phi_\infty)}\right) \tag{9}$$

The bulk correlation length is used to normalize the depth axis since it is roughly the decay length of the SB profile. For this demonstration, we chose samples with ϕ_∞ well below the binodal composition and, thus, far from any wetting transition. The flattened region near the surface is substantial, a third to half of ξ in these low ϕ_∞ samples, and far larger than the dimensions over which long-range forces were seen to influence the shape of the segregation profiles.[29] The NR measurements, with their sensitivity to the near-surface profile, demonstrate that the surface enrichment profile predicted by mean-field theory cannot be correct. That this feature is present at two temperatures over a length scale comparable to the bulk correlation length implies

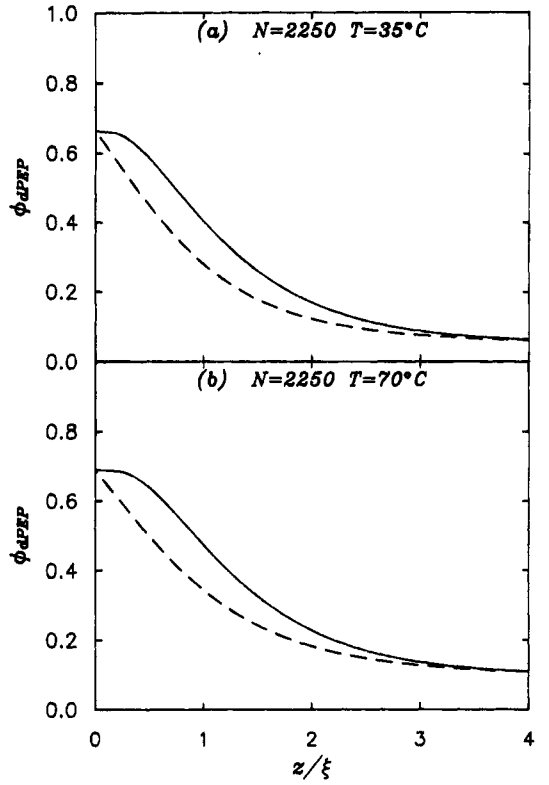

Figure 6. Measured composition profiles (solid lines) scaled by the bulk correlation length ξ for (a) $\Delta x_d = 9.9$, T = 35 °C, $\phi_\infty = 0.054$ and (b) $\Delta x_d = 9.9$, T = 70 °C, $\phi_\infty = 0.099$, where $\xi = a/6[(1-\phi_\infty)/2N_h + \phi_\infty/2N_d - \chi\phi_\infty(1-\phi_\infty)]^{-1/2}$. Dashed lines computed with eq 3.

that correlations ignored by the mean-field theories play a key role in determining the exact structure of the surface-enriched layer. Thus, a non-mean-field theory that accounts for chain conformations and correlations between chains in the surface region will be necessary before a completely satisfactory interpretation of our results is possible.

(2) Surface Energy. Despite the fact that mean-field theory fails to describe the form of the surface segregation profile, the experimental data themselves may be usefully analyzed to give estimates of the surface energy difference between the dPEP and PEP that drives the segregation. One approach is to assume that mean-field theory does not fail too badly and use the SB theory to estimate the bare surface energy derivative $d\gamma_b/d\phi_1$. A second and much less model-dependent approach is to use the Gibbs adsorption equation to extract an estimate of the surface energy difference between dPEP and PEP.

(a) Schmidt–Binder Theory. The effective surface energy difference $d\gamma_b/d\phi_1$ was estimated using eqs 4 and 5 with the experimental values of ϕ_1. In other words, we calculated the $d\gamma_b/d\phi_1$ values that would give the dashed profiles in Figures 2 and 3. The results of this calculation are plotted versus ϕ_1 in Figure 7 with the results from the PEP/dPEP experiments displayed with open circles (70 °C) and open squares (35 °C). For comparison, results are also plotted for PS/dPS from NR experiments[9] (open triangles), where ϕ_1 is measured directly, and from SIMS experiments[10] (open diamonds), where ϕ_1 is computed using the measured z^* and the SB mean-field theory.

It is important to realize that γ_b corresponds only to the bare surface energy term f_s in eq 1; the effects of the square gradient term and the bulk free energy penalty are not included. Nevertheless, because these

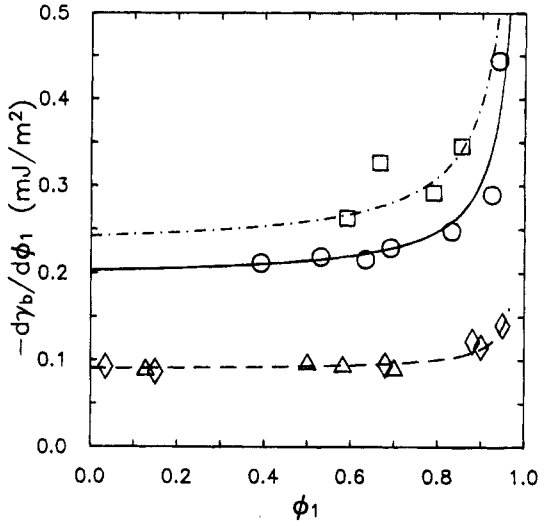

Figure 7. Bare surface energy derivative $d\gamma_b/d\phi_1$, calculated using the SB theory, plotted versus surface volume fraction for neutron reflection measurements of PEP/dPEP samples annealed at 70 °C (circles), for PEP/dPEP annealed at 35 °C (squares), and for PS/dPS (triangles),[9] and (diamonds).[10] The lines are guides to the eye.

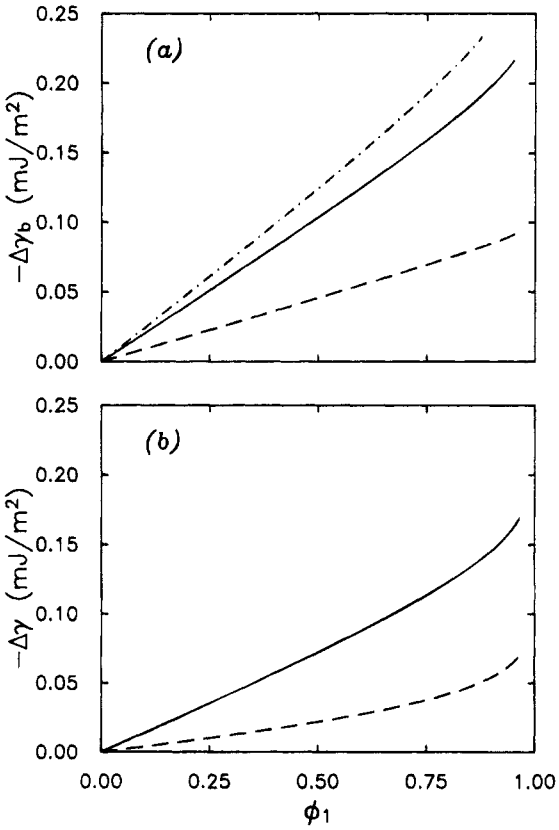

Figure 8. (a) Change in bare surface energy of SB theory extracted by integrating the smoothed data represented by the lines in Figure 7 where the dot-dashed and solid lines are the values for dPEP/PEP at 35 and 70 °C and the dashed line is the values for dPS/PS at 184 °C. (b) Change in surface energy $\Delta\gamma$ of eq 22 from integrating the lines in Figure 9 plotted versus ϕ_1 for PEP/dPEP (solid line) at 35 and 70 °C and PS/dPS (dashed line) at 184 °C.

extra terms do not appear in the surface energy of the pure dPEP and PEP, integrating $d\gamma_b/d\phi_1$ from $\phi_1 = 0$ to 1 gives an estimate of the surface energy difference between the two pure components. Results for PEP/dPEP and PS/dPS are shown in Figure 8a, where we plot $\Delta\gamma_b = \int_0^{\phi_1} d\gamma_b/d\phi_1\, d\phi_1$ as a function of ϕ_1. Note that the surface energy difference between the pure isotopic components (found by extrapolating the curves to $\phi_1 = 1$) appears to be slightly different for the 35 and 70 °C experiments. The values are about 0.27 and 0.23 mJ/m^2 for PEP at 35 and 70 °C, respectively, and ~0.10 mJ/m^2 for PS at 184 °C.

(b) Gibbs Adsorption Equation. The Gibbs adsorption equation offers a method for extracting the surface energy difference without requiring a detailed description, such as the SB theory, of the surface segregation profile. The Gibbs adsorption equation (GAE) is the surface equivalent of the Gibbs–Duhem equation given by

$$d\gamma = -\sum_i \Gamma_i\, d\mu_i \tag{10}$$

where γ is the surface energy, Γ_i is the molecular surface excess of species i, and μ_i is the chemical potential per molecule of species i. In the following discussion we will derive from the GAE an expression for the derivative of the surface energy with respect to the surface composition $d\gamma/d\phi_1$. Combining this expression with the NR data, one can then extrapolate a value for the surface energy difference between the pure components.

In segregation experiments, the integrated surface excess z^* is measured and in a binary mixture of d and h polymers

$$z_d^* + z_h^* = 0 \tag{11}$$

since $\phi_d(z) + \phi_h(z) = 1$, where ϕ_d and ϕ_h are the volume fractions of each species. The molecular surface excess of d is given by

$$\Gamma_d = z_d^* \rho_{d,m}/N_d \tag{12}$$

where $\rho_{d,m}$ is the number of segments of d per unit volume and N_d is the polymerization index of d. From eqs 11 and 12 we see that

$$\frac{\Gamma_d N_d}{\rho_{d,m}} + \frac{\Gamma_h N_h}{\rho_{h,m}} = 0 \tag{13}$$

The segment densities in blends of protonated and deuterated polymers are essentially equal so

$$\Gamma_h = -\Gamma_d\,(N_d/N_h) \tag{14}$$

Thus, for a binary blend of isotopic polymers we can write the GAE as

$$d\gamma = -\Gamma_d\left(d\mu_d - \frac{N_d}{N_h}\, d\mu_h\right) \tag{15}$$

Next we consider the molecular chemical potentials. Relative to the standard state μ_d is given by

$$\frac{\mu_d}{k_B T} = \ln \phi_d + \left(1 - \frac{N_d}{N_h}\right)\phi_h + N_d \chi \phi_h^{\,2} \tag{16}$$

and similarly for h. With some rearrangement and a substitution of $\phi_\infty = \phi_d$ and $1 - \phi_\infty = \phi_h$ we find

$$d\left(\mu_d - \frac{N_d}{N_h}\mu_h\right) = d\left(\ln \phi_\infty - \frac{N_d}{N_h}\ln(1-\phi_\infty) + \left(1 - \frac{N_d}{N_h}\right) + N_d\chi(1 - 2\phi_\infty)\right) \tag{17}$$

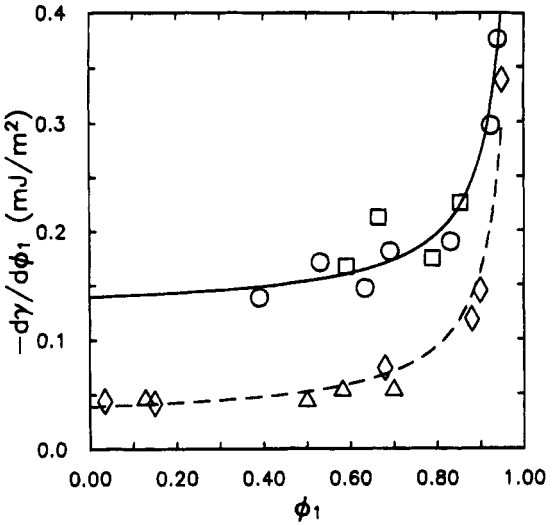

Figure 9. Surface energy derivative $d\gamma/d\phi_1$ derived from the GAE (eq 21) plotted versus the surface volume fraction for PEP/dPEP samples annealed at 70 (circles) and at 35 °C (squares). An estimate of the error is ±20%. Data for PS/dPS from NR and SIMS measurements (triangles)[9] and (diamonds)[10] are also shown. The lines are guides to the eye.

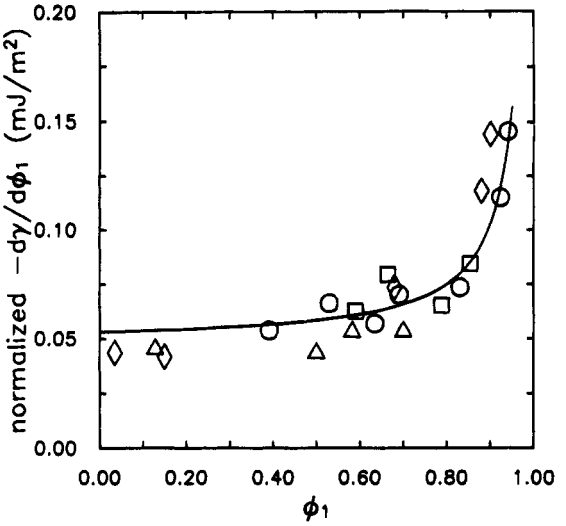

Figure 10. Derivative $d\gamma/d\phi_1$ for each polymer blend normalized by $\Delta\gamma_{blend}/\Delta\gamma_{dPS/PS}$ versus surface volume fraction ϕ_1 where $\Delta\gamma = C(\chi k_B T)^{1/2}$. PEP/dPEP blends annealed at 70 and at 35 °C (circles and squares, respectively), and PS/dPS annealed at 184 °C (triangles[9] and diamonds[10]). The χ for PEP/dPEP was taken from eq 6, and χ for PS/dPS was taken to be 1.5×10^{-4}.[2,10] The line is a guide to the eye.

Now we compute the derivative of the surface energy with respect to the bulk volume fraction. Substituting eqs 12 and 17 into eq 15 and differentiating we find

$$\frac{d\gamma}{d\phi_\infty} = -z^*\rho_m\left(\frac{1}{N_d\phi_\infty} + \frac{1}{N_h(1-\phi_\infty)} - 2\chi\right)k_BT \quad (18)$$

Using eq 9 we rewrite eq 18 as

$$d\gamma/d\phi_\infty = -2z^*\rho_m(\chi_s - \chi)k_BT \quad (19)$$

recognizing that $2(\chi_s - \chi)$ is the second derivative of the Flory–Huggins free energy of mixing per segment.

We would like to find the derivative $d\gamma/d\phi_1$ where ϕ_1 is the surface volume fraction of d. With neutron reflection we measure the ϕ_1 value for each ϕ_∞. We can estimate $d\phi_1/d\phi_\infty$ by fitting a smooth curve to the data of Figure 5. Using this fit we can write

$$\frac{d\gamma}{d\phi_1} = \frac{d\gamma}{d\phi_\infty}\left(\frac{d\phi_1}{d\phi_\infty}\right)^{-1} \quad (20)$$

Combining eq 19 with eq 20 we get

$$\frac{d\gamma}{d\phi_1} = -2\left(\frac{d\phi_1}{d\phi_\infty}\right)^{-1} z^*\rho_m(\chi_s - \chi)k_BT \quad (21)$$

In Figure 9, $d\gamma/d\phi_1$ is plotted versus ϕ_1 for PEP/dPEP and PS/dPS. The trend with ϕ_1 looks much like the $d\gamma_b/d\phi_1$ calculated from the Schmidt and Binder theory (Figure 7). The fact that the magnitude of $d\gamma/d\phi_1$ is smaller than that of $d\gamma_b/d\phi_1$ at $\phi_1 < 0.8$ as well as its more rapid increase as $\phi_1 \rightarrow 1$ is consistent with our expectation that the magnitude of $d\gamma/d\phi_1$ is decreased due to the inclusion of bulk and gradient free energy penalty terms. It is interesting to note, however, that the two separate curves for $d\gamma_b/d\phi_1$ of PEP/dPEP at temperatures of 35 and 70 °C (Figure 7) collapse approximately to one curve for $d\gamma/d\phi_1$ at both temperatures (Figure 9). Since the surface energy difference between dPEP and PEP is not likely to be as strongly temperature dependent as implied by Figure 7, the result shown in Figure 9 seems more physically reasonable.

As we did previously for the SB theory results, we can estimate the surface energy difference between the pure components by integrating the smoothed data on Figure 9 to obtain

$$\Delta\gamma = \int \frac{d\gamma}{d\phi_1}\, d\phi_1 \quad (22)$$

The results for PEP/dPEP and PS/dPS are plotted in Figure 8b. From this figure, the surface energy difference between the pure isotopic components extrapolates to ~0.21 mJ/m^2 for PEP and to ~0.08 mJ/m^2 for PS. These numbers are in reasonable agreement with those extrapolated from the SB theory results (Figure 8a).

Finally, we can compare the difference in surface energy for the dPEP/PEP system $\Delta\gamma = \gamma_{dPEP} - \gamma_{PEP}$ with that for the dPS/PS system. Coarse-grained lattice models that neglect entropic contributions of the chain connectivity and assume van der Waals-type interactions between segments ($\epsilon_{hd} = (\epsilon_{hh}\epsilon_{dd})^{1/2}$) predict that

$$\Delta\gamma = C\sqrt{\chi k_BT} \quad (23)$$

where $C = (fz/b^2)(2/z)^{1/2}(\epsilon_{hh}^{1/2} - \epsilon_{dd}^{1/2})$ with z being the coordination number of the lattice, f the fraction of missing bonds at the surface, and b^2 the surface area per segment. The segment interaction energies are given by ϵ_{ij} where i, j is either an H or D segment.

To test these ideas we have normalized the values of $d\gamma/d\phi_1$ of the dPEP/PEP system by the ratio of $\Delta\gamma_{dPEP/PEP}/\Delta\gamma_{dPS/PS}$ computed as specified by eq 23; the normalization constants are 2.67 and 2.58 for dPEP/PEP at 35 and 70 °C, respectively. These values are plotted in Figure 10 along with the values for dPS/PS (normalization constant, 1). The fact that all the data collapse onto a single curve to within the experimental scatter suggests that the $C(\chi k_BT)^{1/2}$ scaling for $\Delta\gamma$ predicted by eq 23 is reasonable. The fact that PEP/dPEP has a larger $\Delta\gamma$ than PS/dPS derives ultimately from its larger number of C–H (or C–D) bonds per unit volume.

Conclusions

We have investigated segregation to a free surface of the isotopic polymer blend of PEP/dPEP. The surface

enrichment is driven by the small surface energy difference, ~0.21 mJ/m^2, between the hydrogenated and deuterated polymer segments, a consequence of the difference in polarizability of the C−H and C−D bonds that also accounts for the miscibility gap in long-chain isotopic blends. This surface energy difference was extracted from the data using the Gibbs adsorption equation (GAE), a method that is less model dependent than that based on the SB theory used previously. A reason for placing more reliance on the GAE method is that mean-field theories, such as the SB theory, predict segregation profiles that decay approximately exponentially with depth. High-resolution dPEP segment density profiles from neutron reflectometry, however, show features that are in strong disagreement with the mean-field theory predictions. When depth scales of the profiles are scaled by the bulk correlation length ξ, the resulting curves show a layer of nearly constant dPEP concentration before asymptotically approaching the mean-field theory shape at a distance from the surface of about ξ. The characteristic length scale of the deviation is far larger than the range of dispersive forces and is a large fraction of the bulk correlation length. While mean-field theories include the essential physics to predict the qualitative behavior of polymer blends near a free surface, the flattened profile suggests the need to take into account the chain conformations and correlations between chains to explain our results.

Acknowledgment. The authors gratefully acknowledge primary funding from the National Science Foundation Polymer Program NSF-DMR, Grant 922-3099, with additional support for F.S.B. on NSF-DMR Grant 895-7386. L.J.N. was funded in part by a Department of Education Polymer Fellowship. We thank J. Blakely for valuable discussion about the GAE. We thank J. Genzer for comparing our data with his SCF calculations. We also thank D. B. Schwartz, J. Heier, C.-A. Dai, and R. Soave. The reflectivity measurements were done with the help of W. Dozier, K. H. Dai, and G. Krausch at the IPNS at Argonne National Laboratory, which is funded by the U.S. Department of Energy under Contract W-31-109-ENG-38. We benefited from the use of the National Nanofabrication Facility and the facilities of the Materials Science Center at Cornell University both of which are supported by the NSF. Report 7805, issued by the Materials Science Center.

Appendix

The profiles used as input for NR calculations were generated as follows. An exponentially decaying layered concentration profile, which mimics the shape of the SB prediction, was created first as

$$z_{SB}(\phi) = \lambda_1 \log\left(\frac{\phi_1 - \phi_\infty}{\phi - \phi_\infty}\right) \tag{24}$$

between ϕ_1 and $\phi_\infty + 10^{-4}$ with a layer spacing of constant $\Delta\phi$. To deform the profile away from the exponential form, a correction was added

$$z(\phi) = z_{SB} + \mathrm{corr}(z) \tag{25}$$

where

$$\mathrm{corr}(z) = \lambda_{max}[1 - \exp(-(z/\lambda_2)^\beta)] \tag{26}$$

Conversion to $(b/V)(z)$ was done using the scattering length density values in Table 1. The number of layers was chosen to be large enough so that no change in $R(k)$ occurred by decreasing $\Delta\phi$. Parameters used to fit the data are summarized in Tables 2 and 3.

References and Notes

(1) Bates, F. S.; Wignall, G. D.; Koehler, W. C. *Phys. Rev. Lett.* **1985**, *55*, 2425.
(2) Bates, F. S.; Wignall, G. D. *Phys. Rev. Lett.* **1986**, *57*, 1429.
(3) Bates, F. S.; Fetters, L. J.; Wignall, G. D. *Macromolecules* **1988**, *21*, 1086.
(4) Nakanishi, H.; Pincus, P. *J. Chem. Phys.* **1983**, *79*, 997.
(5) Schmidt, I.; Binder, K. *J. Phys. (Paris)* **1985**, *46*, 1631.
(6) For a bare surface energy of the SB form, i.e., $-d\gamma_b/d\phi_1 = \mu_1 + g\phi_1$, the difference between the surface energies of the pure components corresponds to the value of $d\gamma_b/d\phi_1$ at $\phi_1 = 0.5$. Our data, however, do not support the SB form and we will therefore subsequently determine the difference in surface energies by integrating the derivative determined from the experimental data.
(7) Bhatia, Q. S.; Pan, D. H.; Koberstein, J. T. *Macromolecules* **1988**, *21*, 2166.
(8) Schmidt, J. J.; Gardella, J. A., Jr.; Salvati, L., Jr. *Macromolecules* **1989**, *22*, 4489.
(9) Jones, R. A. L.; Norton, L. J.; Kramer, E. J.; Composto, R. J.; Stein, R. S.; Russell, T. P.; Mansour, A.; Karim, A.; Felcher, G. P.; Rafailovich, M. H.; Sokolov, J.; Zhao, Z.; Schwarz, S. A. *Europhys. Lett.* **1990**, *12*, 41.
(10) Zhao, W.; Zhao, X.; Sokolov, J.; Rafailovich, M. H.; Schwarz, S. A.; Wilkens, B. J.; Jones, R. A. L.; Kramer, E. J. *Macromolecules* **1991**, *24*, 5991.
(11) Hariharan, A.; Kumar, S. K.; Russell, T. P. *J. Chem. Phys.* **1993**, *98*, 4163.
(12) Affrossman, S.; Hartshorne, M.; Kiff, T.; Pethrick, R. A.; Richards, R. W. *Macromolecules* **1994**, *27*, 1588.
(13) Hong, P. P.; Boerio, F. J.; Smith, S. D. *Macromolecules* **1994**, *27*, 596.
(14) Gehlsen, M. D.; Rosedale, J. H.; Bates, F. S.; Wignall, G. D.; Hansen, L.; Almdal, K. *Phys. Rev. Lett.* **1992**, *68*, 2452.
(15) Zirkel, A.; Richter, D.; Pyckhout-Hintzen, W.; Fetters, L. J. *Macromolecules* **1992**, *25*, 954.
(16) Frantz, P.; Granick, S. *Langmuir* **1992**, *8*, 1176.
(17) Foster, M. D.; Sikka, M.; Singh, N.; Bates, F. S.; Satija, S. K.; Majkrzak, C. F. *J. Chem. Phys.* **1992**, *96*, 8605.
(18) Kedrowski, C.; Bates, F. S.; Wiltzius, P. *Macromolecules* **1993**, *26*, 3448.
(19) Heier, J.; Krausch, G.; Kramer, E. J.; Bates, F. S., unpublished results.
(20) Felcher, G. P.; Hilleke, R. O.; Hilleke; Crawford, R. K.; Haumann, J.; Kleb, R.; Ostrowski, G. *Rev. Sci. Instrum.* **1987**, *58*, 609.
(21) Russell, T. P. *Mater. Sci. Rep.* **1990**, *5*, 179.
(22) Born, M.; Wolf, E. *Principles of Optics*; Pergamon Press: Oxford, U.K., 1975.
(23) Norton, L. J.; Kramer, E. J.; Jones, R. A. L.; Bates, F. S.; Brown, H. R.; Felcher, G. P.; Kleb, R. *J. Phys. II Fr.* **1994**, *4*, 367.
(24) Zhang, H.; Gallagher, P. D.; Satija, S. K.; Lindstrom, R. M.; Paul, R. L.; Russell, T. P.; Lambooy, P.; Kramer, E. J. *Phys. Rev. Lett.* **1994**, *72*, 3044.
(25) Zhao, W.; Rafailovich, M. H.; Sokolov, J.; Fetters, L. J.; Plano, R.; Sanyal, M. K.; Sinha, S. K.; Sauer, B. B. *Phys. Rev. Lett.* **1993**, *70*, 1453.
(26) Jones, R. A. L.; Norton, L. J.; Kramer, E. J.; Bates, F. S.; Wiltzius, P. *Phys. Rev. Lett.* **1991**, *66*, 1326.
(27) Krausch, G.; Dai, C.-A.; Kramer, E. J.; Bates, F. S. *Macromolecules* **1993**, *26*, 5566.
(28) Chen, Z. Y.; Noolandi, J.; Izzo, D. *Phys. Rev. Lett.* **1991**, *66*, 727.
(29) Jones, R. A. L. *Phys. Rev. E* **1993**, *47*, 1437.
(30) Genzer, J.; Faldi, A.; Composto, R. J. *Phys. Rev. E* **1994**, *50*, 2273.
(31) Genzer, J.; Faldi, A.; Composto, R. J., in preparation
(32) Genzer, J. private communication.
(33) Cohen, S. M.; Muthukumar, M. *J. Chem. Phys.* **1989**, *90*, 5749.
(34) Jerry, R. A.; Nauman, E. B. *J. Colloid Interface Sci.* **1992**, *154*, 122.
(35) Sikka, M.; Singh, N.; Karim, A.; Bates, F. S.; Satija, S. K.; Majkrzak, C. F. *Phys. Rev. Lett.* **1993**, *70*, 307.
(36) Fredrickson, G. H.; Donley, J. P. *J. Chem. Phys.* **1992**, *97*, 8941.

MA950492D